JOURNAL OF VIROLOGY, Aug. 1999, p. 6800–6809 Vol. 73, No. 8
0022-538X/99/$04.00+0

The Murine Cytomegalovirus Chemokine Homolog, m131/129, Is a Determinant of Viral Pathogenicity

PETER FLEMING,[1] NICHOLAS DAVIS-POYNTER,[2] MARIAPIA DEGLI-ESPOSTI,[1] ELOISE DENSLEY,[1] JOHN PAPADIMITRIOU,[3] GEOFFREY SHELLAM,[1] AND HELEN FARRELL[2]*

Departments of Microbiology[1] and Pathology,[3] University of Western Australia, Nedlands, Western Australia 6907, Australia, and Centre for Preventive Medicine, Animal Health Trust, Newmarket CB8 7UU, United Kingdom[2]

Received 10 February 1999/Accepted 15 April 1999

Chemokines are important mediators of the early inflammatory response to infection and modify a wide range of host immune responses. Functional homologs of cellular chemokines have been identified in a number of herpesviruses, suggesting that the subversion of the host chemokine response contributes to the pathogenesis of these viruses. Transcriptional and reverse transcription-PCR analyses demonstrated that the murine cytomegalovirus (MCMV) chemokine homolog, m131, was spliced at the 3′ end to the adjacent downstream open reading frame, m129, resulting in a predicted product of 31 kDa, which is significantly larger than most known chemokines. The in vivo impact of m131/129 was investigated by comparing the replication of MCMV mutants having m131/129 deleted (Δm131/129) with that of wild-type (wt) MCMV. Our studies demonstrate that both wt and Δm131/129 viruses replicated to equivalent levels during the first 2 to 3 days following in vivo infection. However, histological studies demonstrated that the early inflammatory response elicited by Δm131/129 was reduced compared with that of wt MCMV. Furthermore, the Δm131/129 mutants failed to establish a high-titer infection in the salivary glands. These results suggest that m131/129 possesses proinflammatory properties in vivo and is important for the dissemination of MCMV to or infection of the salivary gland. Notably, the Δm131/129 mutants were cleared more rapidly from the spleen and liver during acute infection compared with wt MCMV. The accelerated clearance of the mutants was dependent on NK cells and cells of the $CD4^+$ $CD8^+$ phenotype. These data suggest that m131/129 may also contribute to virus mechanisms of immune system evasion during early infection, possibly through the interference of NK cells and T cells.

Chemokines comprise a large superfamily of chemoattractant cytokines that play an important role in the early inflammatory responses of the host against a wide range of pathogens (39). They have the ability to modulate the movement (chemotaxis) of leukocytes and upregulate the expression of leukocyte adhesion molecules, thus promoting diapedesis and infiltration of cells to the inflammatory site (38). In addition, evidence is accumulating that chemokine production has major sequelae on a wide range of innate and adaptive host immune responses (23).

Members of the chemokine family are structurally similar and are classified according to the arrangement and position of conserved amino-terminal cysteine residues (e.g., C, CC, CXC, or CX3C, where X is any amino acid). They bind to target cells via seven transmembrane domain, G-protein-coupling receptors; the cellular distribution of the receptors determines the leukocyte subset that predominates in different types of inflammation (30). In vitro studies have demonstrated considerable promiscuity in chemokine receptor-ligand interactions. In vivo, it is likely that the nature of the leukocyte recruited to an inflammatory site will depend on both the nature and kinetics of chemokine release.

Chemokines play a critical role in the host response to a number of viruses and in the induction of virus-induced disease (12, 18, 22, 44). The importance of chemokines in the antiviral response has been further implicated by the identification of chemokines and chemokine receptor homologs encoded by a number of large DNA viruses (reviewed in references 29 and 33). Human cytomegalovirus (HCMV), herpesvirus saimiri, human herpesvirus 6 (HHV-6), and HHV-8 each encode a functional chemokine receptor that, like their cellular counterparts, is coupled to G proteins at the cellular membrane (1, 3, 6, 20, 24). Notably, the HCMV chemokine receptor homolog, US28, also serves as a cofactor for human immunodeficiency virus type 1 entry into and fusion of infected cells (34). Unlike other described viral chemokine receptors, the HHV-8 homolog is constitutively active and stimulates cellular proliferation in vitro in the absence of chemokines, suggesting that it may contribute to the transforming potential of HHV-8 in vivo (3). Putative chemokine receptors have also been identified in both murine and rat CMV (MCMV, RCMV) (5, 35) and have been shown to be virulence factors in vivo (5, 14). In both mouse herpesvirus 68 and equine herpesvirus 2, homologs to chemokine receptors have been found, although their contribution to pathogenesis remains to be determined (43, 45). In addition to the above homologs of cell surface chemokine receptors, a soluble CC chemokine binding protein (vCKBP) encoded by poxviruses has been shown to block the biologic activity of chemokines in vitro and in vivo (2, 22, 41). Furthermore, the myxoma virus gamma interferon receptor homolog (M-T7) nonspecifically sequesters CC and CXC chemokines via a heparin binding domain (27, 31). This additional function of M-T7 is consistent with an increased inflammatory response in rabbits infected with a myxoma virus mutant lacking M-T7.

Two functional CC chemokine homologs, designated vMIP-1 and vMIP-II (32), are encoded by HHV-8; the latter exhibits broad-spectrum antagonistic activity to cellular chemokines and inhibits the chemokine-induced chemotaxis of monocytes (25). Interest in these viral chemokines increased when they were shown to partially inhibit HIV infection through the binding of CC and (in the case of vMIP-II) CXC chemokine re-

* Corresponding author. Mailing address: Centre for Preventive Medicine, Animal Health Trust, Lanwades Park, Kentford, Newmarket, Suffolk CB8 7UU, United Kingdom. Phone: 44-1638-750659. Fax: 44-1638-750794. E-mail: helen.farrell@aht.org.uk.

ceptors (7) that can function as coreceptors for HIV (10, 15). Unlike their cellular counterparts, both vMIP-I and vMIP-II are highly angiogenic in vitro, suggesting that they may contribute to the pathology of Kaposi's sarcoma, a condition that is strongly linked to HHV-8 infection (7). The *MC148* gene of the poxvirus molluscum contagiosum virus encodes a CC chemokine homolog (26, 40) that also exhibits a broad-spectrum antagonistic activity against cellular chemokines (13); the protracted replication of molluscum contagiosum virus in the absence of a host inflammatory response may thus be promoted by the *MC148* gene product. Among the human betaherpesviruses, HCMV encodes at least three chemokine homologs (8), and sequence homologs have also been identified in HHV-6 (21). Notably, the HCMV chemokine homologs have been detected in low-passage clinical isolates and are absent from the attenuated, tissue culture-adapted strain, AD169, suggesting that they encode virulence factors.

Since chemokines are likely to be pivotal during early antiviral inflammatory responses, it is presumed that virus homologs of chemokines and chemokine binding proteins may enable the virus to evade or disarm the normal host inflammatory response. For poxviruses, this has been supported by in vivo studies of poxvirus mutants with chemokine binding proteins deleted, which have each been shown to elicit a more vigorous inflammatory response than wild-type (wt) virus (22, 29). Thus, natural animal models of infection provide useful settings to characterize the impact of viral pathogenic determinants.

MCMV contains an open reading frame (ORF) designated m131 whose product has homology with CC chemokines (28). In this report, we demonstrate that the m131 ORF is spliced at the 3′ end to the downstream m129 ORF, producing a protein with predicted mass of 31 kDa, which is larger than known cellular CC chemokines (7 to 15 kDa). The biological significance of m131/129 in the MCMV life cycle in vivo was addressed by comparing the pathogenesis of wt MCMV with that of MCMV mutants containing a m131 ORF that either is disrupted with a *lacZ* cassette (Δm131Z) or contains an introduced in-frame premature stop codon (Δm131ns). While the Δm131Z and Δm131ns virus mutants established an acute in vivo infection comparable to wt virus, they were cleared more rapidly from these sites of infection. Furthermore, these mutants showed reduced replication in the salivary gland, which is the major site of virus persistence and transmission. Histological examination of the spleens and livers of infected animals showed that wt MCMV elicited a more vigorous inflammatory response than did Δm131Z, suggesting that m131/129 may possess proinflammatory properties in vivo. Depletion of natural killer (NK) and $CD4^+$ $CD8^+$ T cells in vivo restored virus titers in the spleens and livers of Δm131Z-infected mice to levels equivalent to or approaching that of wt MCMV but did not modify the reduced replication of Δm131Z in the salivary gland. These results provide the first report of the biological impact of a herpesvirus chemokine in the context of a natural in vivo infection. Our data demonstrate that m131/129 promotes the recruitment of inflammatory leukocytes to the spleen and liver and efficient dissemination to, or replication in, the salivary gland during wt MCMV infection, suggesting that it is a potential chemokine agonist. Our data also demonstrate that m131/129 interferes with the early NK- and T-cell responses of the host, causing protracted replication in primary sites of infection.

MATERIALS AND METHODS

Cells. Primary mouse embryo fibroblasts (MEF) were grown in minimal essential medium supplemented with antibiotics and 10% newborn calf serum. YAC-1 lymphoma cells were cultivated in suspension in RPMI supplemented with antibiotics and 10% fetal calf serum.

Mice. Specific-pathogen-free, age-matched 6- to 8-week-old BALB/c mice were obtained from the Animal Resource Centre, Murdoch, Australia, and maintained under minimal disease conditions.

Virus. The virulent MCMV strain K181 Perth was used as the wt virus for these studies, and all recombinant viruses were derived from this strain. The Perth strain is derived from and has a restriction enzyme pattern similar to that published for the K181 strain, but it has been passaged in vivo in this laboratory over a number of years. All master stocks of wt MCMV used in this study were derived from a low-passage stock. wt and mutant viruses were propagated and subjected to titer determination on MEF as previously described (14). For in vivo studies, virus stocks were propagated in the salivary glands of 3-week-old BALB/c mice.

Preparation of MCMV DNA. MEF were infected with MCMV at a multiplicity of infection of 3 to 5. When the cells exhibited an extensive cytopathic effect, infected-cell DNA was prepared as described previously (14).

Preparation of RNA. For the preparation of wt and mutant MCMV RNA, confluent monolayers of MEF were infected with the relevant virus at a multiplicity of infection of 5. Infections were performed in the presence of either cycloheximide (50 μg/ml) or phosphonoacetic acid (250 μg/ml), and the cells were harvested 4 h postinfection (p.i.) corresponding to immediate-early (IE) and early (E) stages of MCMV infection. For the production of late RNA transcripts, MEF were infected in the absence of metabolic inhibitors and harvested at 24 h p.i. All RNAs were prepared by the method of Chomczynski and Sacchi (11).

Northern blot analysis. RNA samples (5 μg) were subjected to electrophoresis under denaturing conditions, blotted onto nylon, and hybridized with [^{32}P]dCTP-labelled double-stranded DNA probes as previously described (14). The genomic location (indicated in kilobase pairs) of ORFs spanning the m131 region and the location of subgenomic fragments used as probes for Northern analysis are shown in Fig. 1A.

Synthesis, cloning, and sequencing of m131/129 cDNA. Following first-strand cDNA synthesis with poly d(T), the m131/129 cDNAs were amplified by PCR with oligonucleotides PF1 (CGGAATTCTAGAATGGGAACGCTCCTCGTG TGCTG) and PF2 (TATGAATTCTTATTCATCGGACAGTCGTTG) and *Pfu* polymerase (Stratagene). The RT-PCR products were digested with *Eco*RI, cloned into pcDNA3 (Invitrogen), and sequenced.

Plasmid constructs. The derivation of plasmids used in this study is shown schematically in Fig. 1B. Genomic clones were derived from the K181 Perth Strain of MCMV and were kindly provided by A. Scalzo (Department of Microbiology, University of Western Australia). An *Eco*RV fragment (nucleotides 186244 to 189836) was subcloned into the *Pvu*II site of pGEM to generate plasmid pGEM131/129, which contains the m131 ORF with approximately 1.6 kb of flanking MCMV sequence. The *lacZ* expression cassette containing the HCMV IE promoter and poly(A) sites was derived from pMV10 (19); the blunt-ended *Hin*dIII fragment of pMV10 was cloned into the filled *Not*I site within the m131 ORF to generate plasmid pGEMm131Z, which was used in transfections with wt MCMV DNA to generate Δm131*lacZ*$^+$ recombinants (hereafter designated Δm131Z). Restriction analysis of pGEMm131Z confirmed that the *lacZ* cassette was inserted in the opposite orientation to the m131 ORF. For the generation of an MCMV mutant containing a premature stop codon in the m131 ORF, (hereafter referred as Δm131ns), the oligonucleotide pair (5′G GCCTAATTAGCTGATATC3′ and 5′GGCCGATATCAGCTAATTA3′) was inserted into the *Not*I site of pGEMm131 to generate plasmid pGEMm131ns. This insertion introduced a unique *Eco*RV site that was used to identify the presence of the oligonucleotide pair. In addition, the region flanking the *Not*I insertion site was sequenced to confirm the correct insertion of the oligonucleotide pair.

Transfection. Transfection of MEF was performed on subconfluent monolayers in 35-mm dishes by the method of Chen and Okayama (9). Monolayers were transfected with 10 μg of infected-cell MCMV DNA plus 3 to 6 μg of the plasmid DNA of interest, using previously described methods (14). For the identification of recombinant viruses expressing β-galactosidase, plaques were stained with 5-bromo-4-chloro-3-indolyl-β-D-galactopyranoside (X-Gal). Blue plaques were picked and cloned by at least three rounds of limiting dilution. For the generation of revertant (m131r) and Δm131ns viruses, subconfluent MEF were cotransfected with Δm131Z infected-cell DNA and either pGEMm131 (m131r) or pGEM131ns (Δm131ns). Plaques resulting from the transfection were stained with X-Gal, and "white" (i.e., β-galactosidase-negative) plaques were picked and cloned as above.

Southern blot analysis. Infected-cell DNA was prepared from wt MCMV- or recombinant MCMV-infected MEF. Following digestion with either *Eco*RV or *Sac*I, the DNA was separated on a 1% agarose gel and transferred to nylon by standard methods. The probes used were specific for either the MCMV m131 region or *lacZ*. DNA fragments were gel purified prior to radiolabelling and use in hybridization experiments as specified by the manufacturer (Bresatec, Adelaide, Australia).

In vitro growth of wt and recombinant viruses. Multistep growth curves for wt and recombinant MCMVs were determined in MEF as described previously (14).

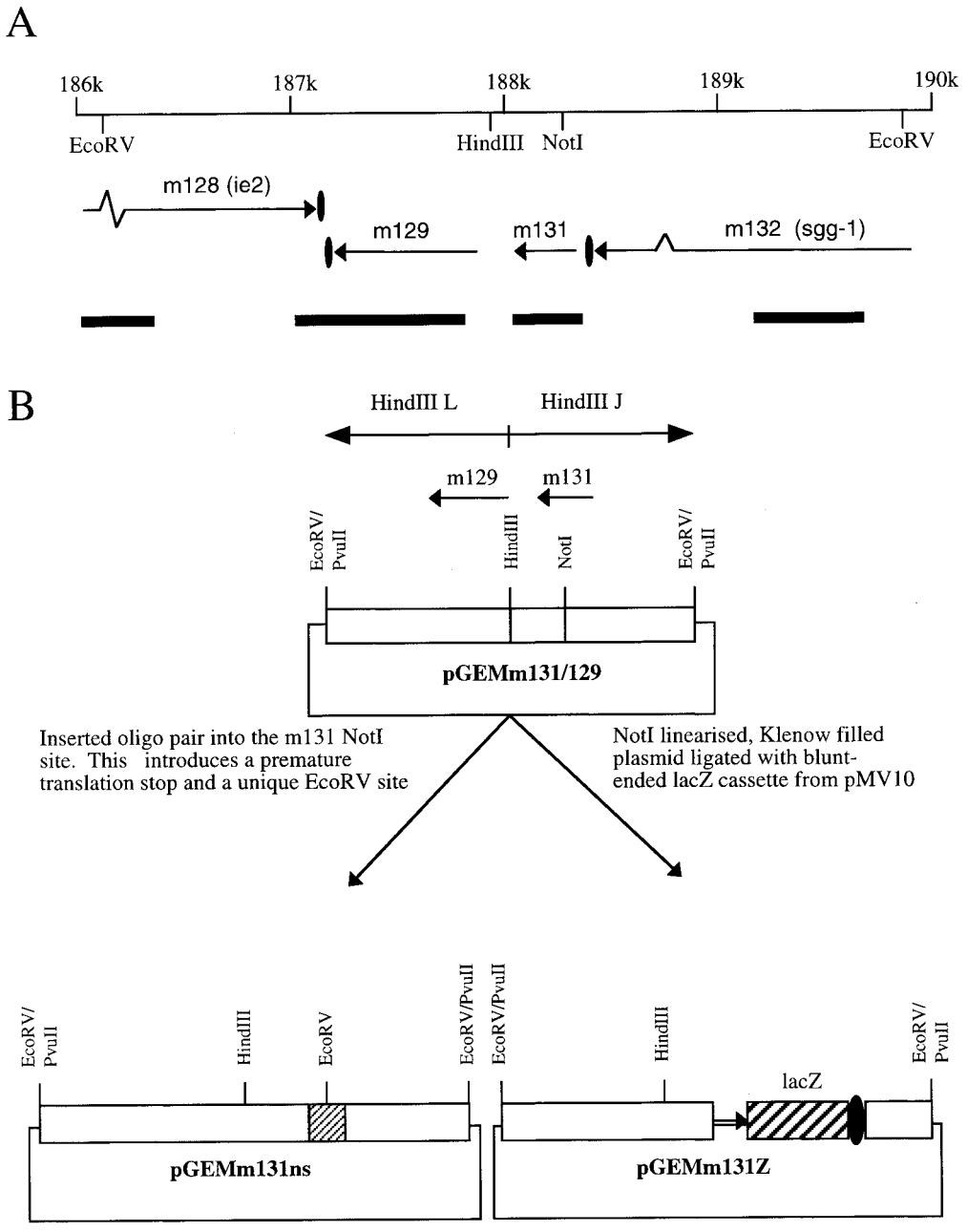

FIG. 1. (A) Genetic organization of the MCMV m131 region. Nucleotide positions refer to the sequenced Smith strain of MCMV. Solid ellipses indicate the position of poly(A) signals on each strand. The specificities of subgenomic fragments used as probes in Northern hybridizations are depicted as solid bars below the ORFs. The probe for the m131 ORF was amplified by PCR from viral DNA. (B) Construction diagrams (not drawn to scale) for plasmids used in this study. Additional details are provided in the text.

In vivo growth of wt and recombinant viruses. Mice were inoculated with wt, recombinant, or revertant viruses by the intraperitoneal (i.p.) route. At designated times p.i., mice were sacrificed and their spleens, livers, and/or salivary glands were removed. All organs were individually weighed, homogenized in cold minimal essential medium supplemented with 2% newborn calf serum and centrifuged at 2,000 × *g* at 4°C. The supernatant was stored at −80°C, and the virus titer was subsequently determined on MEF.

In vivo depletion of cellular subsets. (i) During acute infection. In vivo depletion of $CD4^+$ $CD8^+$ T lymphocytes was performed by i.p. inoculation of BALB/c mice with both YTS 169.4 and YTS 191.1 cytotoxic monoclonal antibodies on days −1 and +2 relative to MCMV infection. Confirmation of T-cell depletion was determined on day 4 by fluorescence-activated cell sorter (FACS) analysis with rat monoclonal antibodies 3.168.8 (anti-CD8) and RL-172 (anti-CD4). Specific binding was detected with a fluorescent secondary antibody; nonspecific binding (background) was assessed by incubating cells with normal rat serum followed by the secondary antibody. Binding of the detecting antibodies used in the FACS analysis was not inhibited by the presence of the cytotoxic antibodies used for the in vivo depletion. In vivo depletion of NK cells was performed by i.p. inoculation of anti-asialo GM_1 on days −1 and +2 relative to MCMV infection. NK-cell depletion was confirmed on day +4 by NK assay of splenocytes in a standard 4-h chromium release assay with YAC-1 cells as targets.

(ii) During persistent infection. Mice were depleted of either NK cells or $CD4^+$ $CD8^+$ T cells on days +7 and +9 relative to MCMV infection by using the above antibodies, and the salivary glands were harvested on day +11 p.i. Depletion of NK cells and $CD4^+$ $CD8^+$ T cells were confirmed by the method described above on day +10 p.i.

Histological testing. Spleen and liver samples from wt- and Δm131Z-infected mice and uninfected mice were harvested on day 2 p.i., incubated in Bouin's

fixative for 16 h, and mounted in paraffin. Sections were cut and stained with hemotoxylin and eosin. The number of inflammatory foci was counted in at least 10 liver sections. The number of nucleated inflammatory cells per focus of infection was derived by counting the number of cells around at least 20 foci taken at random.

GenBank accession number. The sequence of m131/129 strain K181 (Perth) has been assigned accession no. AF124602.

RESULTS

Characterization of recombinant MCMV with a disrupted m131 ORF. To investigate the biological significance of m131, MCMV recombinants in which the m131 coding region had been disrupted by insertion of the *lacZ* expression cassette (Δm131Z) or the introduction of an in-frame stop codon (Δm131ns) were constructed and characterized (Fig. 1B). A revertant virus was also generated from one of the *lacZ*-positive recombinants as described in Materials and Methods. Following three rounds of plaque purification, stocks of each recombinant and revertant were prepared and DNA from virus-infected cells was analyzed by Southern blot hybridization. Three Δm131Z recombinants were cloned from independent transfections; all were analyzed by Southern blot hybridization, and the correct insertion of *lacZ* was confirmed. Two of these recombinants were further analyzed in vitro and in vivo (as described below) and found to possess identical phenotypes. However, for simplicity, genetic and phenotypic analysis of one *lacZ* recombinant (Δm131Z), from which the revertant, m131r, and premature translation stop mutant, Δm131ns, were derived, are presented here. Figure 2 shows the result of Southern blot analysis of the recombinant viruses in comparison with wt MCMV. All samples were digested with *Eco*RV and *Sac*I and hybridized to probes specific for either the m131 region or *lacZ*. The bands observed for the Δm131Z and Δm131ns recombinants are as predicted following the insertion of either the *lacZ* cassette or the oligonucleotide pair respectively, and there is no evidence of contaminating wt virus, confirming that the stocks are clonally pure. The bands observed for m131r were identical to those for wt MCMV, demonstrating that the wt profile had been rescued and that it, too, was clonally pure.

Transcriptional analysis of the m131 region in the Δm131Z and Δm131ns recombinant viruses. To confirm that the coding sequences flanking m131 had not been disrupted by the insertion of *lacZ* into Δm131Z, RNA harvested at IE, E, and late (L) times from wt- and Δm131Z-infected cells was subjected to Northern analysis with probes specific for m128 (*ie2*), m129, m131, and m132 (*sgg1*). Consistent with previous studies (28), m131 was expressed as a late transcript of approximately 1 kb in wt MCMV; insertion of the 3.8-kb *lacZ* cassette resulted in a larger (>4-kb) species in the Δm131Z recombinant (Fig. 3). Notably, m129 was also expressed in wt MCMV as a late 1-kb transcript, which was not detected in Δm131Z, indicating that m131 and m129 may comprise a single transcriptional unit (see below). Transcription from the upstream adjacent gene, m132, appeared to be unaffected by the *lacZ* insertion, as was that from the 1.8-kb m128 (*ie2*) gene. A novel RNA species (>6 kb) identified at IE times for Δm131Z was shown to hybridize to *lacZ* and is thus likely to represent readthrough of *ie2* through to the *lacZ* poly(A). However, this represents a minor species in comparison with the authentic *ie2* transcript. Northern analysis of Δm131ns showed these recombinants to be identical to wt, demonstrating that the insertion of the oligonucleotide pair had not disrupted transcription in this region.

m131 and m129 are expressed as a single spliced transcript. Given that both m131 and m129 are encoded by 1-kb transcripts expressed with the same kinetics and that both transcripts are disrupted by *lacZ*, we investigated the possibility

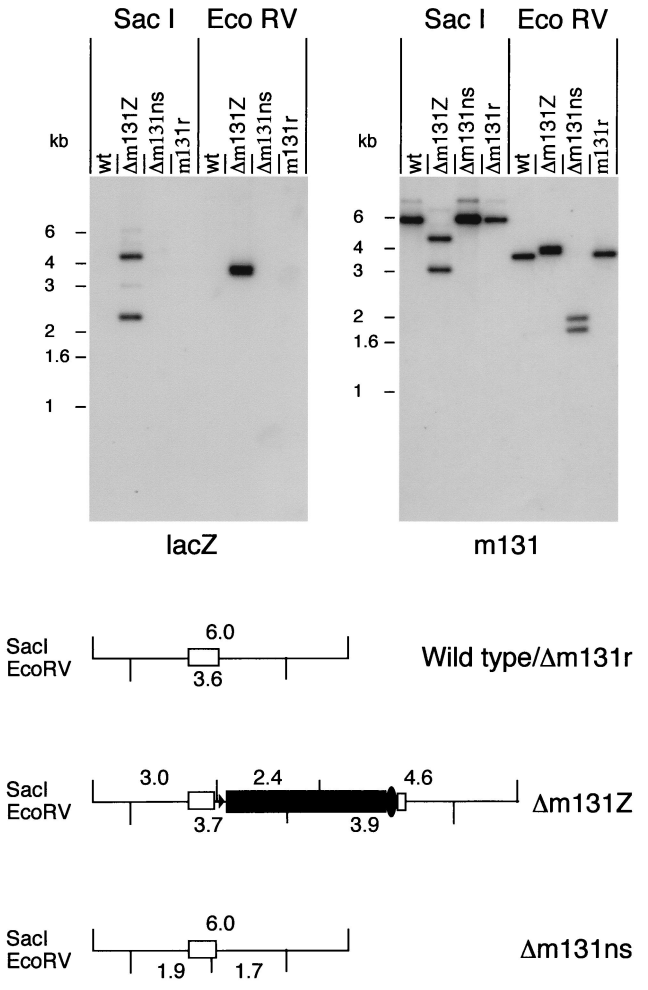

FIG. 2. Southern blot analysis of MCMV recombinants. DNA samples were prepared from cells infected with either wt, Δm131Z, Δm131ns, or m131r virus. Samples were digested with *Sac*I or *Eco*RV, separated on a 1.0% agarose gel, and blotted onto nylon membranes before being hybridized to radiolabelled probes. The 3.8-kb *lacZ* cassette from pMV10 (19) was used as the *lacZ* probe; the m131 probe was derived from genomic MCMV DNA by PCR. The predicted positions of *Sac*I and *Eco*RV sites for each of the viruses are shown schematically below the blot. The open boxes represent the m131 ORF. The solid box represents the *lacZ* ORF. Predicted fragment sizes are indicated in kilobases.

that m131 and m129 were expressed as a single, spliced transcription unit. Analysis of the sequences of m131 and m129 ORFs showed a putative splice donor site at the 3′ end of m131 (immediately upstream of the translational stop codon) and a putative splice acceptor site 100 bp upstream of the initial ATG within m129. Reverse transcription-PCR (RT-PCR) analysis of RNA from wt MCMV was performed with primers for first- and second-strand synthesis as described in Materials and Methods. The size of the RT-PCR product was compared with that of the corresponding PCR product by using infected-cell DNA as the template. While a single PCR product of the predicted size was observed, the RT-PCR product was approximately 100 bp shorter. The RT-PCR product was cloned into pGEM-T (Promega), and several clones were selected for sequencing. The results of the sequencing confirmed the existence of the spliced mRNA. The sequence of the spliced product, the identified splice junctions, and the 82-bp intron sequence are shown in Fig. 4. The m129 DNA sequence of the Perth strain differs slightly from that of the published Smith

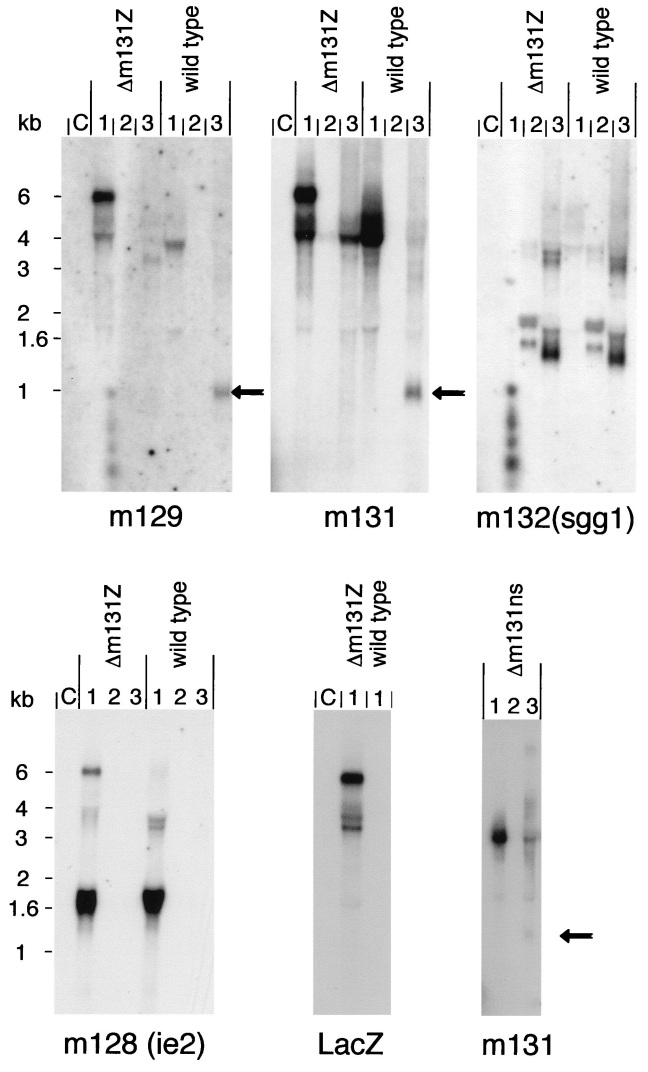

FIG. 3. Northern blot analysis of RNA isolated from MCMV-infected MEF at immediate-early (lanes 1), early (lanes 2), and late (lanes 3) times p.i. RNA from uninfected MEF was included as a control. Total RNA (5 μg) was separated in a denaturing agarose gel, blotted onto nylon, and hybridized with double-stranded DNA probes. The specificity of the DNA probes is indicated in Fig. 1A. Solid arrows denote the 1-kb m131/129 transcript in wt MCMV and in Δm131ns.

```
      M  G  T  L  L  V  C  C  L  V  C  C  V  V  L  V  V  S  T  V
01    ATGGGAACGCTCCTCGTGTGCTGCCTCGTCTGTTGCGTCGTGTTGGTCGTGTCTACCGTC
      A  D  L  R  E  P  C  C  A  R  P  Q  L  H  P  L  P  L  Y  A
61    GCGGACCTCCGCGAGCCATGTTGCGCCGCCGCCGCAGCTGCACCCTCTCCCGCTGTACGCG
      V  Q  S  A  E  Y  T  N  T  S  C  G  R  E  V  V  F  T  T  F
121   GTACAGAGCGCCGAATACACTAACACTTCGTGCGGACGAGAGGTGGTTTTCACTACCTTC
      S  G  M  R  V  C  A  K  R  A  W  W  S  D  R  L  L  C  L  V
181   TCTGGGATGAGGGTGTGCGCTAAGCGGGCCTGGTGGTCGGACAGACTCTTGTGTCTGGTC
      R  *
241   AGgtgagtgttttgatctgaaaggagagggatcggcgggggggcgcgataggggatgtctg
                                  S  R  S  D  S  R  L  R  V  L  L  I
301   atctgtgtgtctgtgtgtatatagATCTCGGTCAGATTCCAGACTGCGTGTCCTGCTTAT
        F  G  E  L  L  K  A  F  N  T  T  I  K  L  V  P  V  D  P  A
361   CTTTGGTGAGCTACTGAAAGCTTTCAACACCACCATCAAGCTCGTGCCCGTGGACCCCGC
        D  M  M  Y  V  A  D  V  M  T  E  S  P  R  I  T  V  G  K  Y
421   CGACATGATGTACGTGGCCGATGTGATGACAGAATCGCCACGCATCACGGTGGGCAAGTA
        P  Y  E  V  K  D  G  E  N  W  I  E  C  V  C  E  I  T  W  V
481   CCCCTACGAGGTGAAGGACGGTGAAAACTGGATAGAGTGTGTCTGTGAGATCACCTGGGT
        G  N  G  T  N  W  P  L  G  I  H  P  F  K  P  T  V  W  I  Q
541   CGGGAACGGTACGAACTGGCCGCTCGGCATACATCCGTTCAAACCCACGGTGTGGATACA
        Y  T  L  Q  V  T  F  S  G  K  D  N  D  P  S  S  R  C  I  N
601   GTACACGTTGCAGGTGACGTTCTCCGGCAAGGATAACGACCCCTCCTCACGCTGCATCAA
        S  S  H  V  S  E  R  R  W  T  V  D  P  P  E  R  L  L  D  F
661   CAGCTCGCACGTGTCCGAGAGACGGTGGACCGTGGATCCCCCCGAGAGATTGTTAGACTT
        N  Q  Y  V  A  T  L  L  S  S  A  S  P  P  T  G  A  A  K  T
721   CAACCAGTACGTAGCAACTTTATTATCCTCGGCCTCCCCCCCTACCGGCGCAGCAAAAAC
        L  L  T  P  T  A  V  E  C  E  F  K  N  A  S  E  T  L  R  T
781   TTTATTAACCCCCACGGCGGTAGAGTGCGAGTTCAAGAACGCATCCGAGACACTCAGGAC
        P  Y  Y  C  M  P  L  T  S  G  E  P  P  P  G  R  V  F  Y  R
841   ACCATACTACTGCATGCCCCTCACATCGGGGGAACCCCCTCCGGGGCGAGTCTTTTACAG
        L  Q  R  L  S  D  E  *
901   GCTACAACGACTGTCCGATGAATGA      922
```

FIG. 4. Nucleotide sequence of the splice junction determined for MCMV m131/129. The intron sequences are displayed in lowercase type. Changes in the nucleotide and amino acid sequence from the published Smith strain are underlined; the cysteine residues conserved with cellular CC chemokines and the predicted initiating methionine residues for m131 and m129 are doubly underlined. The *Not*I site used for the insertion of the *lacZ* cassette and oligonucleotide pair is underscored by a dashed line. The predicted signal sequence and N-linked glycosylation sites (N-X-T/S, where X is any amino acid) are shown in italics.

strain and has only one nonconservative amino acid change. No changes in the m131 sequence were detected. The predicted m131/129 protein is much larger than most known cellular chemokines; the C-terminal half of the protein that is contributed by m129 does not possess a predicted transmembrane or anchor sequences, and thus it is unlikely that m131/129 is a membrane glycoprotein.

m131/129 is not required for replication in fibroblasts in vitro. Multistep growth curves were generated to determine whether the mutation in m131 affected the growth of the recombinant virus in cell culture. Primary MEF were infected with either wt MCMV or Δm131Z at a multiplicity of infection of 0.01, and virus titers were determined at various times p.i. (Fig. 5). No significant difference in replication between wt K181 and Δm131Z was observed, indicating that m131/129 is not important for growth in fibroblasts in vitro.

In vivo characterization of recombinant MCMV. To address the biological significance of m131/129, the ability of Δm131Z to replicate in vivo was compared with that of wt MCMV. Figure 6 represents the results from one of three separate challenges of BALB/c mice infected i.p. with 10^4 PFU of either wt MCMV or Δm131Z. Virus titers in the spleen, liver, and salivary glands were determined at various time points p.i. The two viruses were equally effective in establishing infections in the spleen and liver to high titer by day 2 p.i., suggesting that m131/129 is not critical for the initial rounds of replication in these organs. Notably, the clearance of Δm131Z from the spleen and liver was accelerated compared with that of wt MCMV. In addition, Δm131Z was significantly attenuated in its ability to establish a high-titer persistent infection in the salivary glands, with virus titers being ca. 10^3-fold lower than those of wt virus. Results from in vivo replication studies of m131r showed that it replicated to wt levels in the spleen and liver during the acute phase and subsequently in the salivary glands, confirming that the Δm131Z phenotype was attributed

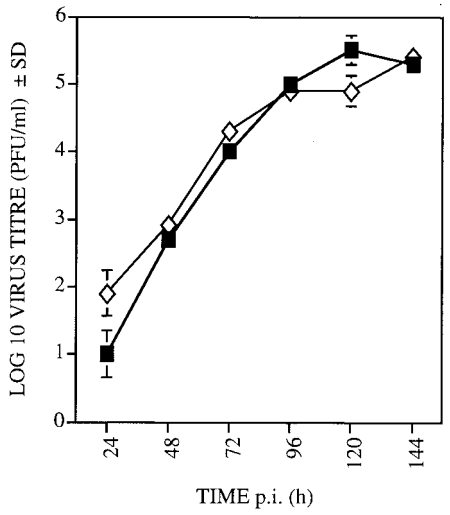

FIG. 5. Multistep growth curves of wt MCMV and Δm131Z in MEF. Confluent monolayers were infected with 0.01 PFU of either wt (■) or Δm131Z (◇) virus per cell. Following virus adsorption (1 h at 37°C), monolayers were washed, fresh medium was added, and the mixture was incubated for various time points before the cells and supernatant were harvested. Samples were stored at −80°C before being used for titer determination on MEF. Each point represents the $\log_{10}$ of the mean PFU per milliliter, with one standard deviation, of triplicate samples. The in vitro growth rates of m131r and Δm131ns were also shown to be similar to those of wt virus and are not presented in the figure.

to the disruption of the m131 ORF rather than to adventitious mutations elsewhere in the MCMV genome (data not shown). To further establish a role for m131/129 in the early and persistent replication of MCMV in vivo, the growth of Δm131ns was compared with that of m131r and Δm131Z in BALB/c mice. Like the Δm131Z mutant, the Δm131ns mutant was cleared more rapidly than m131r in the spleen and liver during acute infection and failed to establish a high-titer infection in the salivary glands (Fig. 7).

Accelerated clearance of Δm131Z during acute infection is mediated by T cells and NK cells. Given that Δm131Z and Δm131ns were cleared more rapidly from the spleen and liver during acute infection than was wt MCMV, we investigated whether this was due to an altered ability of the host to combat the virus during this period rather than to a defect in the ability of mutant viruses to spread from cell to cell within these organs. The timing of the clearance of the virus mutants is consistent with a heightened T-cell response. Accordingly, the role of $CD4^+$ $CD8^+$ T-lymphocyte populations in this accelerated clearance was assessed by using the Δm131Z mutant. Although protection mediated by NK cells is usually observed by day 2 p.i., when wt and mutant viruses exhibit equivalent titers, the role of NK cells in the clearance of Δm131Z was also assessed. Mice depleted in vivo of either NK cells or $CD4^+$ $CD8^+$ lymphocytes (as described in Materials and Methods) were infected with wt MCMV or the Δm131Z mutant. Virus titers were determined on day 5 p.i., the time when the most significant differences in virus titers in the spleen and liver between wt-infected and Δm131Z-infected mice were reproducibly observed in immunocompetent mice. The efficacy and specificity of the NK-cell and $CD4^+$ $CD8^+$-T-cell depletion regimens were assessed on day 4 p.i. (data not shown). NK-cell depletion was assessed by measuring the NK-cell activity of splenocytes with YAC-1 targets in a standard 4-h lysis assay. In vivo depletion of asialo GM_1-positive cells reduced the levels of NK activity in wt- and Δm131Z-infected mice to the level

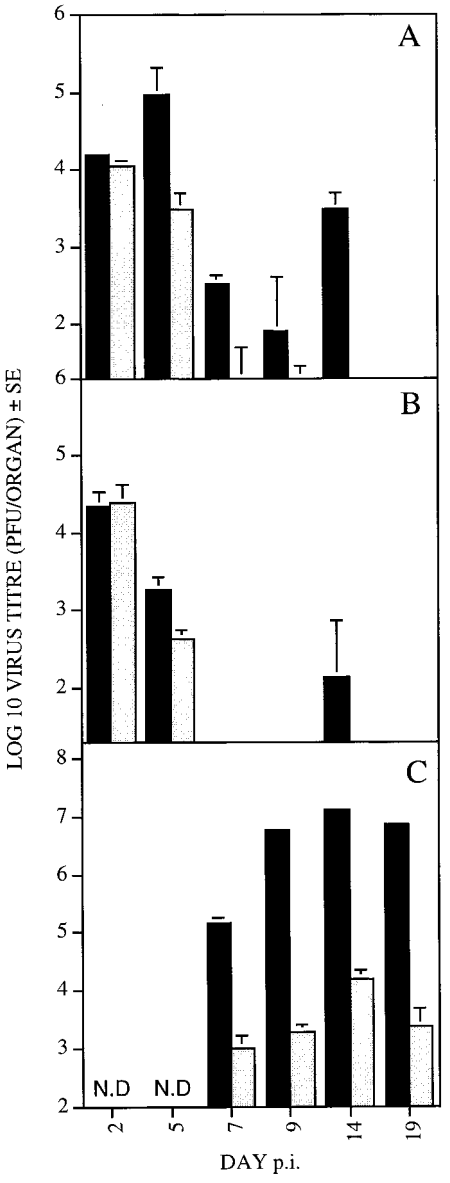

FIG. 6. Growth of wt (black bars) and Δm131Z (grey bars) virus in the spleens (A), livers (B), and salivary glands (C). Groups of four BALB/c mice were infected i.p. with 10^4 PFU of the relevant virus, and spleens, livers, and salivary glands were harvested on the days indicated. Organs were homogenized and stored at −80°C before being used for titer determination on MEF. Virus titers are expressed as mean $\log_{10}$ per organ, with standard error. The *y* axis is cropped to indicate the lower limit of virus detection. N.D, not determined.

observed in control (uninfected) animals. In addition, the depletion of $CD4^+$ $CD8^+$ T cells did not affect the NK-cell activity in these groups. The efficacy of $CD4^+$ $CD8^+$-T-cell depletion was assessed by analyzing the profile of $CD4^+$ and $CD8^+$ lymph node cells by FACS analysis on day 4 p.i. The percentage of cells positive for CD4 and CD8 markers was reduced to background levels (as described in Materials and Methods) in depleted animals but was unaffected by anti-asialo GM_1 treatments.

The effects of NK-cell and $CD4^+$ $CD8^+$-T-cell depletion on replication of wt MCMV and Δm131Z in the spleen and liver are shown in Fig. 8A and B. As expected, Δm131Z-infected immunocompetent mice sustained a significantly lower titer of

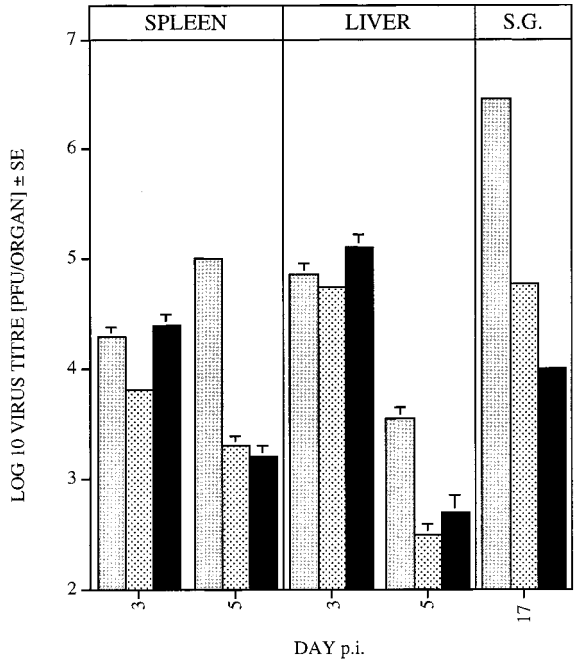

FIG. 7. Growth of m131r (shaded bars), Δm131ns (stippled bars), and Δm131Z (solid bars) in vivo. Groups of four BALB/c mice were infected i.p. with 10^4 PFU of the relevant virus. Organs were harvested and homogenized on the days indicated and stored at −80°C before being used for titer determination on MEF. Virus titers are expressed as the mean $\log_{10}$ per organ, with standard error. The *y* axis is cropped to indicate the lower limit of virus detection. S.G., salivary glands.

virus in the spleen and liver than did wt-infected mice. In the spleen, neither NK- nor $CD4^+$ $CD8^+$-T-cell depletion caused increased titers in wt-infected mice, consistent with previous studies (17). However, in Δm131Z-infected animals, NK- and $CD4^+$ $CD8^+$-T-cell depletion resulted in elevated titers of virus in the spleen, equivalent to the titers in wt-infected animals. NK and $CD4^+$ $CD8^+$ depletions caused increases in the virus titer of Δm131Z in the liver that were in excess of those observed for wt-infected mice. Taken together, these results demonstrate that restriction of virus replication by NK cells or $CD4^+$ $CD8^+$ T cells contributes to the observed attenuation of Δm131Z during acute infection of immunocompetent animals.

Neither NK cells nor $CD4^+$ $CD8^+$ T cells contribute to the restricted replication of Δm131Z in the salivary gland. To determine whether NK cells or $CD4^+$ $CD8^+$ T cells restrict the replication of Δm131Z in the salivary gland, mice were depleted of either of these cell subsets 7 days p.i. and the salivary glands were harvested on day 11 p.i. This time point was chosen for immune system depletion since it corresponded to the time of virus clearance from the spleen and liver and the initiation of virus replication in the salivary gland. Immune system depletion prior to MCMV infection was not possible in this study, since this leads to overwhelming titers in the spleen and liver prior to the full establishment of virus replication in the salivary glands and is accompanied by high morbidity and mortality rates.

The Δm131Z mutant exhibited restricted replication in both immune system-depleted and immunocompetent animals, demonstrating that the attenuated phenotype of Δm131Z in the salivary glands is not due to enhanced NK-cell- or $CD4^+$ $CD8^+$-T-cell-mediated control of virus replication (Fig. 8C).

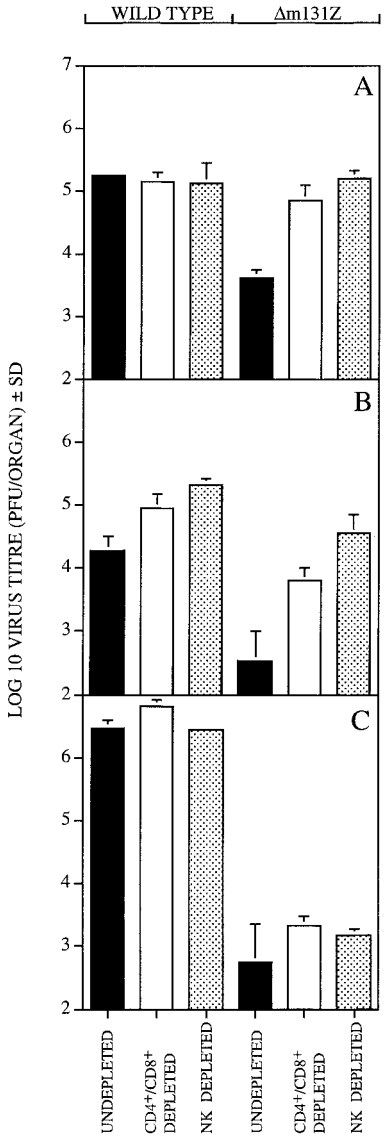

FIG. 8. Effect of NK-cell and $CD4^+$ $CD8^+$-T-cell depletion on the replication of wt and Δm131Z in the spleen (A), liver (B) and salivary gland (C). The methods used for in vivo depletion of NK cells (stippled bars) and $CD4^+$ $CD8^+$ T cells (open bars) is described in the text. Undepleted mice (solid bars) were used as controls. All mice received $10^{4.3}$ PFU of either wt or Δm131Z. Virus titers in the spleen and liver were determined on day 5 p.i.; virus titers in the salivary gland were determined in a separate study on day 11 p.i. Each group represents the $\log_{10}$ of the mean PFU per organ, with one standard deviation, from five mice. The *y* axis is cropped to indicate the lower limit of virus detection.

Histological comparison of wt and Δm131Z infections in vivo. Previous studies have shown that MCMV induces an early focal inflammation in the liver and spleen following intraperitoneal infection. To characterize the contribution of m131/129 to the inflammatory responses, samples were isolated from infected mice on day 2 p.i., when mutant and wt viruses replicate to equivalent levels. Tissue sections were prepared and stained with hematoxylin and eosin for morphological analyses of the inflammatory response. In the liver, wt-infected tissues exhibited a larger number of inflammatory foci (29 ± 3) than did Δm131Z-infected tissues (14 ± 2). Furthermore, when the numbers of leukocytes around each focus of infection were compared (Fig. 9), it was noted that foci in

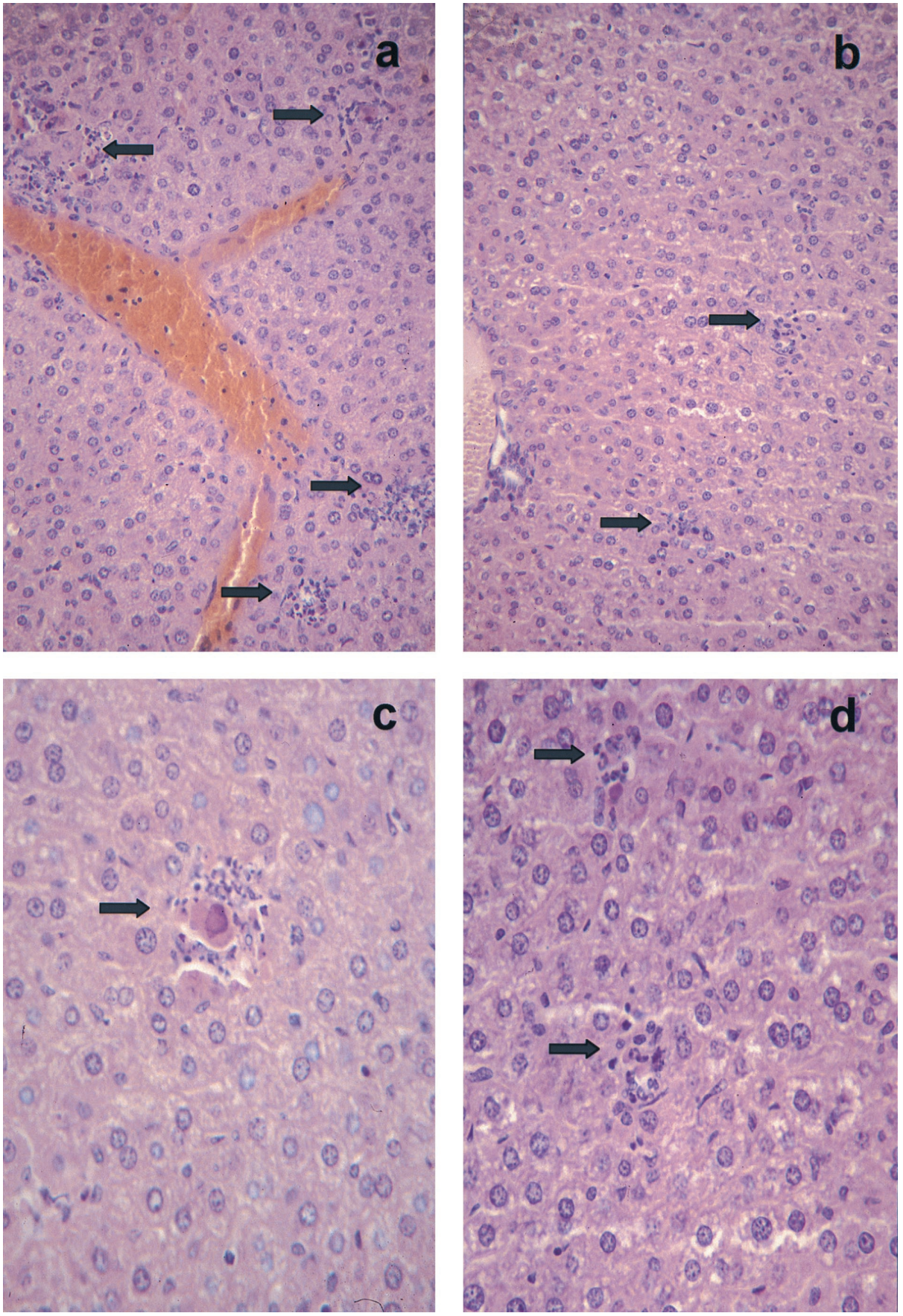

FIG. 9. Δm131Z elicits a reduced inflammatory infiltrate in the livers of infected mice. Samples were prepared from livers of wt- and Δm131Z-infected BALB/c mice harvested 2 days p.i. (a and b) The number of foci of infection observed for the wt (a) and recombinant (b) viruses. Magnification, ×22.75. Foci of infection are marked by arrows. (c and d) The number of inflammatory cells surrounding each focus of infection for the wt (c) and Δm131Z (d) viruses. Magnification, ×36.4.

wt-infected tissues contained more inflammatory cells (26 ± 3) than did foci in Δm131Z-infected tissues (14 ± 3). These findings suggest that m131/129 promotes an early inflammatory response and recruits cells to the sites of infection.

DISCUSSION

Chemokines and their receptors are common targets for subversion or exploitation by persistent viruses, demonstrating their importance in the host response to virus infection. Since homologs of chemokines and chemokine receptors are widespread among the gamma- and betaherpesviruses, they may provide a function that is intrinsic to the in vivo life cycle of these herpesvirus subfamilies. Since a distinguishing feature of the gamma- and betaherpesviruses is their ability to replicate in leukocytes, it is perhaps not surprising that these subgroups encode proteins that have the potential to modify leukocyte homeostasis. Possible functions of viral chemokines and/or chemokine receptors include (i) the attraction of uninfected leukocytes to the site of infection (recruitment of susceptible targets), (ii) the trafficking of infected leukocytes to sites of protracted virus shedding (virus dissemination and transmission), (iii) the binding of virus to specific cell types (virus tropism), and (iv) the blocking of host chemokine-dependent mechanisms of virus clearance (immune evasion).

We have examined the biological significance of the putative MCMV CC chemokine homolog by comparing the dissemination of wt MCMV with MCMV mutants with an intact *m131/129* ORF deleted. The results of this study indicate that m131/129 may possess both proinflammatory and immune system-evasive properties.

First, histological examination of wt- or Δm131Z-infected organs showed that m131/129 contributed to the early recruitment of inflammatory cells to the spleen and liver. Since MCMV replication is highly cell associated (42), it is possible that m131/129 acts as a chemokine agonist, recruiting leukocytes that provide a source of susceptible targets. Recent evidence has shown that m131 elicits a calcium flux with a proinflammatory role (36). Studies are in progress to identify the cells comprising the inflammatory infiltrate and to determine their susceptibility to MCMV infection.

In comparison with wt MCMV, both Δm131Z and Δm131ns mutants exhibited reduced titers in the salivary glands of infected animals. This restricted dissemination was shown to be independent of host NK cells or $CD4^+$ $CD8^+$ T lymphocytes. Thus, it is possible that m131/129 plays a role in either virus dissemination to or infection of the salivary glands. Notably, the putative MCMV chemokine receptor, encoded by *M33*, and its counterpart in RCMV (*R33*) play a critical role in salivary gland tropism. Given that the salivary gland is a major site of CMV transmission, it would be anticipated that the retention of ORFs that encode determinants of MCMV growth in salivary glands would provide a selective advantage in the natural setting. Indeed, sequence analysis of tissue culture-adapted HCMV strains AD169 and Towne has shown that these strains lack a considerable portion of the genome, including the chemokine homologs, that is present in the recent clinical Toledo strain. Sequence analysis of multiple field isolates of MCMV has shown that the chemokine receptor homolog, *M33*, is highly conserved (16); similarly, it would be of interest to determine whether m131/129 is also conserved.

Second, our studies demonstrated that although virus titers in the spleens and livers of Δm131Z, Δm131ns, and wt-infected animals were equivalent on day 2 p.i., the mutant viruses were cleared more rapidly. This rapid clearance was dependent on the NK-cell and (to a lesser extent) the $CD4^+$ $CD8^+$ T-cell compartment. Recent studies have shown that the cellular CC chemokine, MIP-1α, recruits NK cells to the liver as early as days 2 and 3 following MCMV infection (37). Given the homology of m131/129 to cellular CC chemokines, it is tempting to suggest that m131/129 interferes with the chemokine-dependent pathways of NK-cell- and T-cell-mediated virus clearance. Given the proinflammatory properties of m131/129, it may recruit cells to sites of infection that downregulate NK-cell and T-cell function. Alternatively, m131/129 may directly block NK- and T-cell activation or modulate cell surface adhesion molecules that are important for effector-target conjugate formation.

While first described as inducible mediators of inflammation, chemokines are now known to play a pivotal role in the shaping of the innate and adaptive immune system responses to infection. The results of our in vivo studies suggest that m131/129 may interfere with the early events in the host cellular response to MCMV infection, thus contributing to protracted virus replication and improved virus dissemination within the host. Taken together, our data suggest contrasting agonist and antagonist roles for m131/129, namely, increased recruitment of leukocytes to foci of infection together with inhibition of NK- and T-cell-mediated clearance. Such proinflammatory and inhibitory properties have also been described for the HHV-8 CC chemokine homolog, vMIP-II, which is a potent chemoattractant for eosinophils yet blocks the chemotaxis of monocytes (25).

Transcriptional analysis of the m131 region has identified a number of spliced ORFs. Spliced late herpesvirus transcripts are uncommon, and in this respect the m131/129 spliced transcript is unusual. Cellular CC chemokines are also spliced, with a conserved structure comprising three exons, but none of the intron-exon boundaries are positioned similarly to m131/129. The product of m131/129 has a predicted mass of 31K, which is significantly larger than that of most other known cellular chemokines. The only cellular chemokine that has a similar mass to m131/129 is the membrane-bound CX_3C chemokine, fractalkine (4). Unlike fractalkine, however, m131/129 is not predicted to be membrane bound. The significance of the contribution of m129 to the function of m131/129 is uncertain, since the homology of m131/129 to CC chemokines is located entirely within the m131 ORF and m129 does not have homology to other sequences in the published databases. Future structure-function studies will be important to evaluate the contribution of the m129 moiety to the function of m131/129.

It is now apparent that MCMV possesses multiple genes that contribute to virulence, either by interfering with host immune responses or by modifying virus dissemination and/or tropism. To our knowledge, this is the first demonstration that a herpesvirus chemokine homolog can modulate the early cell-mediated immune response in vivo. Since chemokine homologs are present in a number of herpesviruses that lack suitable in vivo models, the analysis of these and other conserved virulence genes in MCMV provides a valuable biological system to determine the role of these genes in infection of the natural host.

ACKNOWLEDGMENTS

The provision of MCMV strain K181 (Perth) genomic clones and antibodies to NK and T lymphocyte subsets by Tony Scalzo, University of Western Australia, is gratefully acknowledged. We also thank the Department of Pathology, University of Western Australia, for the preparation of histological sections.

This project was supported by the National Health and Medical Research Council of Australia and the Animal Health Trust, United Kingdom. N.D.-P. was supported by a Tetra Laval Fellowship.

REFERENCES

1. **Ahuja, S. K., and P. M. Murphy.** 1993. Molecular piracy of mammalian interleukin 8 receptor type B by herpesvirus saimiri. J. Biol. Chem. **268:** 20691–20694.
2. **Alcami, A., J. A. Symons, P. D. Collins, T. J. Williams, and G. L. Smith.** 1998. Blockade of chemokine activity by a soluble chemokine binding protein from vaccinia virus. J. Immunol. **160:**624–633.
3. **Arvanitakis, L., E. Geras-Raaka, A. Varma, M. C. Gershengorn, and E. Cesarman.** 1997. Human herpesvirus KSHV encodes a constitutively active G protein-coupled receptor linked to cell proliferation. Nature **385:**347–350.
4. **Bazan, J. F., K. B. Bacon, G. Hardiman, W. Wang, K. Soo, D. Rossi, D. R. Greaves, A. Zlotnik, and T. J. Schall.** A new class of membrane-bound chemokine with a CX_3C motif. Nature **385:**640–644.
5. **Beisser, P. S., C. Vink, J. G. Van Dam, G. Grauls, S. J. V. Vanherle, and C. A. Bruggeman.** 1998. The R33 G protein-coupled receptor gene of rat cytomegalovirus plays an essential role in the pathogenesis of viral infection. J. Virol. **72:**2352–2363.
6. **Billstrom, M. A., G. L. Johnson, N. J. Avdi, and G. S. Worthen.** 1998. Intracellular signalling by the chemokine receptor US28 during human cytomegalovirus infection. J. Virol. **72:**5535–5544.
7. **Boshoff, C., Y. Endo, P. D. Collins, Y. Takeuchi, J. D. Reeves, V. L. Schweickart, M. A. Siani, T. Sasaki, T. J. Williams, P. W. Gray, P. S. Moore, Y. Chang, and R. A. Weiss.** 1997. Angiogenic and HIV-inhibitory functions of KSHV-encoded chemokines. Science **278:**290–294.
8. **Cha, T. A., E. Tom, G. W. Kemble, G. M. Duke, E. S. Mocarski, and R. R. Spaete.** 1996. Human cytomegalovirus clinical isolates carry at least 19 genes not found in laboratory strains. J. Virol. **70:**78–83.
9. **Chen, C., and H. Okayama.** 1987. High-efficiency transformation of mammalian cells by plasmid DNA. Mol. Cell. Biol. **7:**2745–2752.
10. **Choe, H., M. Farzan, Y. Sun, N. Sullivan, B. Rollins, P. D. Ponath, L. Wu, C. R. Mackay, G. LaRosa, W. Newman, N. Gerard, C. Gerard, and J. Sodroski.** 1996. The beta-chemokine receptors CCR3 and CCR5 facilitate infection by primary HIV-1 isolates. Cell **85:**1135–1148.
11. **Chomczynski, P., and N. Sacchi.** 1987. Single step method of RNA isolation by acid guanidium thiocyanate-phenol-chloroform extraction. Anal. Biochem. **162:**156–159.
12. **Cook, D. N., M. A. Beck, T. M. Coffman, S. L. Kirby, J. F. Sheridan, I. B. Pragnell, and O. Smithies.** 1995. Requirement of MIP-1α for an inflammatory response to viral infection. Science **269:**1583–1585.
13. **Damon, I., P. M. Murphy, and B. Moss.** 1998. Broad spectrum chemokine antagonistic activity of a human poxvirus chemokine homolog. Proc. Natl. Acad. Sci. USA **95:**6403–6407.
14. **Davis-Poynter, N. J., D. M. Lynch, H. Vally, G. R. Shellam, W. D. Rawlinson, B. G. Barrell, and H. E. Farrell.** 1997. Identification and characterization of a G protein-coupled receptor homolog encoded by murine cytomegalovirus. J. Virol. **71:**1521–1529.
15. **Doranz, B. J., J. Rucker, Y. Yi, R. J. Smyth, M. Samson, S. C. Peiper, M. Parmentier, R. G. Collman, and R. W. Doms.** 1996. A dual-tropic primary HIV-1 isolate that uses fusin and the beta-chemokine receptors CKR5, CKR3, and CDKR-2b as fusion cofactors. Cell **85:**1149–1158.
16. **Farrell, H. E.** Unpublished data.
17. **Farrell, H. E., H. Vally, D. M. Lynch, P. Fleming, G. R. Shellam, A. A. Scalzo, and N. J. Davis-Poynter.** 1997. Inhibition of natural killer cells by a cytomegalovirus MHC class I homologue in vivo. Nature **386:**510–514.
18. **Fauci, A. S.** 1996. Host factors and the pathogenesis of HIV-induced disease. Nature **384:**529–534.
19. **Forrester, A., H. Farrell, G. Wilkinson, J. Kaye, N. Davis-Poynter, and T. Minson.** 1992. Construction and properties of a mutant of herpes simplex virus type with glycoprotein H coding sequences deleted. J. Virol. **66:**341–348.
20. **Gao, J.-L., and P. Murphy.** 1994. Human cytomegalovirus open reading frame US28 encodes a functional β-chemokine receptor. J. Biol. Chem. **269:**28539–28542.
21. **Gompels, U. A., J. Nicholas, G. Lawrence, M. Jones, B. J. Thomson, M. E. D. Martin, S. Efstathiou, M. Craxton, and H. A. Macaulay.** 1995. The DNA sequence of human herpesvirus-6: structure, coding content and genome evolution. Virology **209:**29–51.
22. **Graham, K. A., A. S. Lalani, J. L. Macen, T. L. Ness, M. Barry, L. Liu, A. Lucas, I. Clark-Lewis, R. W. Moyer, and G. McFadden.** 1997. The T1/35kDa family of poxvirus-secreted proteins bind chemokines and modulate leukocyte influx into virus-infected tissues. Virology **229:**12–24.
23. **Hedrick, J. A., and A. Zlotnik.** 1996. Chemokines and lymphocyte biology. Curr. Opin. Immunol. **8:**343–347.
24. **Isegawa, Y., Z. Ping, K. Nakano, N. Sugimoto, and K. Yamanishi.** 1998. Human herpesvirus 6 open reading frame U12 encodes a functional β-chemokine receptor. J. Virol. **72:**6104–6112.
25. **Kledal, T. N., M. M. Rosenkilde, F. Coulin, G. Simmons, A. H. Johnsen, S. Alouani, C. A. Power, H. R. Luttichau, J. Gerstoft, P. R. Clapham, I. Clark-Lewis, T. N. C. Wells, and T. W. Schwartz.** 1997. A broad-spectrum chemokine antagonist encoded by Kaposi's sarcoma-associated herpesvirus. Science **277:**1656–1659.
26. **Krathwohl, M. D., R. Hromas, D. R. Brown, H. E. Broxmeyer, and K. H. Fife.** 1997. Functional characterization of the C---C chemokine-like molecules encoded by molluscum contagiosum virus types 1 and 2. Proc. Natl. Acad. Sci. USA **94:**9875–9880.
27. **Lalani, A. S., K. Graham, K. Mossman, K. Rajarathnam, I. Clark-Lewis, D. Kelvin, and G. McFadden.** 1997. The purified myxoma virus gamma interferon receptor homolog M-T7 interacts with the heparin-binding domain of chemokines. J. Virol. **71:**4356–4363.
28. **MacDonald, M. R., X. Li, and H. W. Virgin IV.** 1997. Late expression of a β chemokine homolog by murine cytomegalovirus. J. Virol. **71:**1671–1678.
29. **McFadden, G., A. Lalani, H. Everett, P. Nash, and X. Xu.** 1998. Virus-encoded receptors for cytokines and chemokines. Semin. Cell. Dev. Biol. **9:**359–368.
30. **Moser, B., M. Loetscher, L. Piali, and P. Loetscher.** 1998. Lymphocyte responses to chemokines. Int. Rev. Immunol. **16:**323–344.
31. **Mossman, K., P. Nation, J. Macen, M. Garbutt, A. Lucas, and G. McFadden.** 1996. Myxoma M-T7, a secreted homolog of the interferon-γ receptor, is a critical virulence factor for the development of myxomatosis in European rabbits. Virology **215:**17–30.
32. **Nicholas, J., V. R. Ruvolo, W. H. Burns, G. Sandford, X. Wan, D. Ciufo, S. B. Hendrickson, H. Guo, G. S. Hayward, and M. S. Reitz.** 1997. Kaposi's sarcoma-associated human herpesvirus-8 encodes homologs of macrophage inflammatory protein-1 and interleukin-6. Nat. Med. **3:**287–292.
33. **Pease, J. E., and P. M. Murphy.** 1998. Microbial corruption of the chemokine system: an expanding paradigm. Semin. Immunol. **10:**169–178.
34. **Pleskoff, O., C. Treboute, A. Brelot, N. Heveker, M. Seman, and M. Alizon.** 1997. Identification of a chemokine receptor encoded by human cytomegalovirus as a cofactor for HIV-1 entry. Science **276:**1874–1878.
35. **Rawlinson, W. D., H. E. Farrell, and B. G. Barrell.** 1996. Analysis of the complete DNA sequence of murine cytomegalovirus. J. Virol. **70:**8833–8849.
36. **Saederup, N., Y. C. Lin, T. Schall, and E. Mocarski.** 1998. Murine cytomegalovirus (MCMV) β chemokine, (MCK-1), plays a role as a determinant of viremia and dissemination, abstr. p. 249. *In* Abstracts of the 23rd International Herpesvirus Workshop 1998.
37. **Salazar-Mather, T. P., J. S. Orange, and C. A. Biron.** 1998. Early murine cytomegalovirus (MCMV) infection induces liver natural killer (NK) cell inflammation and protection through macrophage inflammatory protein 1a (MIP-1a)-dependent pathways. J. Exp. Med. **187:**1–14.
38. **Schall, T. J., and K. B. Bacon.** 1994. Chemokines, leukocyte trafficking, and inflammation. Curr. Opin. Immunol. **6:**865–873.
39. **Schluger, N. W., and W. N. Rom.** 1997. Early responses to infection: chemokines as mediators of inflammation. Curr. Opin. Immunol. **9:**504–508.
40. **Senkovich, T. G., J. J. Bugert, J. R. Sisler, E. V. Koonin, G. Darai, and B. Moss.** 1996. Genome sequence of human tumorigenic poxvirus: prediction of specific host response-evasion genes. Science **273:**813–816.
41. **Smith, C. A., T. D. Smith, P. J. Smolak, D. Friend, H. Hagen, M. Gerhart, L. Park, D. J. Pickup, D. Torrance, K. Mohler, K. Schooley, and R. G. Goodwin.** 1997. Poxvirus genomes encode a secreted, soluble protein that preferentially inhibits beta chemokine activity yet lacks sequence homology to known chemokine receptors. Virology **236:**316–327.
42. **Stoddart, C. A., R. D. Cardin, J. M. Boname, W. C. Manning, G. B. Abenes, and E. S. Mocarski.** 1994. Peripheral blood mononuclear phagocytes mediate dissemination of murine cytomegalovirus. J. Virol. **68:**6243–6253.
43. **Telford, E. A. R., M. S. Watson, H. C. Aird, J. Perry, and A. J. Davison.** 1995. The DNA sequence of equine herpesvirus 2. J. Mol. Biol. **249:**520–528.
44. **Teruya-Feldstein, J., E. S. Jaffe, P. R. Burd, H. Kanegane, D. W. Kingma, W. H. Wilson, D. L. Longo, and G. Tosato.** 1997. The role of Mig, the monokine induced by interferon-γ, and IP10, the interferon-γ inducible protein-10, in tissue necrosis and vascular damage associated with Epstein-Barr virus-positive lymphoproliferative disease. Blood **90:**4099–4105.
45. **Virgin IV, H. W., P. Latreille, P. Wamsley, K. Hallsworth, K. E. Weck, A. J. Dal Canto, and S. H. Speck.** 1997. Complete sequence and genomic analysis of murine gammaherpesvirus 68. J. Virol. **71:**5894–5904.